Available online at www.sciencedirect.com
ScienceDirect
International Journal of Heat and Mass Transfer 51 (2008) 4820–4828
International Journal of HEAT and MASS TRANSFER
www.elsevier.com/locate/ijhmt

Prediction of radiative heat transfer between two concentric spherical enclosures with the finite volume method

Man Young Kim [a,*], Seung Wook Baek [b], Chang Yeop Lee [c]

[a] Department of Aerospace Engineering, Chonbuk National University, 664-14 Duckjin-Dong, Duckjin-Gu, Jeonju, Chonbuk 561-756, Republic of Korea
[b] Department of Aerospace Engineering, Korea Advanced Institute of Science and Technology, Taejon 305-701, Republic of Korea
[c] Manufacturing System Center, Korea Institute of Industrial Technology, Cheonan, Chungnam 330-825, Republic of Korea

Received 26 July 2007; received in revised form 21 February 2008
Available online 7 April 2008

Abstract

The radiative heat transfer between two concentric spheres separated by an absorbing, emitting, and isotropically scattering gray medium is investigated by using the finite volume method (FVM). Especially, a mapping that simplifies the solution of spherically symmetric radiative heat transfer problems is introduced, thereby, the intensity depending on spatial one-dimension and angular one-dimension is transformed into spatial two-dimensional one. By adopting this mapping process, angular redistribution, which appears in such curvilinear coordinates as cylindrical or spherical ones, is treated efficiently without any artifice usually introduced in the conventional discrete ordinates method (DOM). After a mathematical formulation and corresponding discretization equation for the radiative transfer equation (RTE) are derived, final discretization equation is introduced by using the directional weight, which is the key parameter in the FVM since it represents the inflow or outflow of radiant energy across the control volume faces depending on its sign. The present approach is then validated by comparing the present results with those of previous works by changing such various parameters as temperature ratio between inner and outer spherical enclosure, wall emissivity, and optical thickness of the participating medium. All the results presented in this work show that the present method is accurate and valuable for the analysis of spherically symmetric radiative heat transfer problems between two concentric spheres.

Keywords: Radiative heat transfer; Finite volume method; Spherically symmetric coordinate; Mapping process; Directional weight

1. Introduction

For many engineering applications such as droplet combustion, spherical reacting systems, and droplet radiator systems for spacecraft thermal control, spherically symmetric assumption is usually made due to its geometric and theoretical simplicity and thereby economic benefits because it physically describes three-dimensional phenomena with one-dimensional procedure. Therefore, a substantial effect has been exerted to analyze the spherically symmetric problems in the field of radiation as well as flow and heat transfer including combustion [1–7]. During the past few decades, numerous methods have been proposed to solve the RTE between two concentric spheres separated by radiatively active medium. Among others, while Viskanta and Crosbie [1] considered a nonscattering, gray, and heat-generating medium between two concentric spheres with the differential approximations, Tsai et al. [2] investigated the thermal radiation in spherical symmetry with anisotropic scattering and variable properties by using the DOM. Jia et al. [3] extended the Galerkin method to investigate the radiative heat transfer between two concentric spheres separated by an absorbing, emitting and isotropically scattering gray medium. Especially, while Sghaier et al. [4] and Trabelsi et al. [5] developed a new method for the solution of the RTE in spherical media based on the DOM with finite Legendre transform (FLT) to model the angular derivative term, Aouled-Dlala et al. [6] introduced the finite Chebyshev transform (FCT) with the DOM for the analysis of

* Corresponding author. Tel.: +82 63 270 2473; fax: +82 63 270 2472.
E-mail address: manykim@chonbuk.ac.kr (M.Y. Kim).

0017-9310/$ - see front matter © 2008 Elsevier Ltd. All rights reserved.
doi:10.1016/j.ijheatmasstransfer.2008.02.016

Nomenclature

a_I^m	coefficient of the discretization equation in direction m at nodal point I
D_i^m	directional weight in direction m at surface i, Eqs. (4) and (7)
$D_i^{m\pm1/2}$	angular edge directional weight in direction $m \pm 1/2$ at surface i, Eq. (5), $i = e$ and w
D_r^m	directional weight in direction m at the surface normal to r-direction, Eq. (7)
E, W, N, S	east, west, north, and south neighbor control volume of P, respectively, see Fig. 3
e, w, n, s	east, west, north, and south face of the control volume of P, respectively, see Fig. 3
$\vec{e}_r, \vec{e}_\theta, \vec{e}_\varphi$	r-, θ-, φ- direction base vectors, respectively
I	radiative intensity, [W(m^2 sr)]
I_b	blackbody radiative intensity, $= \sigma T^4/\pi$, [W(m^2 sr)]
$\vec{n}_i$	outward unit normal vector at face i
$\vec{n}_w$	unit normal vector at the wall towards the medium
P	present control volume
q_r^R	radial radiative heat flux, [W/m^2], Eq. (1)
$\vec{r}$	position vector
$\vec{s}$	direction vector, $= \vec{e}_r \cos\chi + \vec{e}_\theta \sin\chi \sin\omega + \vec{e}_\varphi \sin\chi \cos\omega$
w^m	angular weight in the DOM, Eq. (14)

Greek Symbols

$\alpha^{m\pm1/2}$	coefficients of the angular derivative term, Eq. (14)
β	extinction coefficient, $= \kappa_a + \sigma_s$, [m^{-1}]
χ	angular polar angle measured from the r-axis, see Fig. 1
χ_0	spatial polar angle measured from the right horizontal line, see Fig. 2
$\Delta A, \Delta V$	surface area and volume of the control volume, respectively
$\Delta\Omega^m$	discrete control angle, [sr]
ε_w	wall emissivity
κ_a, σ_s	absorption and scattering coefficients, respectively, [m^{-1}]
μ	direction cosine in the r-direction, $= \cos\chi$, see Fig. 1
ω	angular azimuthal angle measured from the θ-axis

Subscripts

1,2	inner and outer spherical walls, respectively, see Fig. 1
w	wall

Superscripts

m	radiation direction

combined conductive and radiative heat transfer in concentric spherical medium. Recently, Kim et al. [7] proposed the modified DOM by adopting the control angle concepts usually used in the FVM, and demonstrated the benchmark solutions of radiative heat transfer between two concentric spheres filled with nongray gas and particle mixture.

As a neutron travels through a curved geometry such as cylindrical or spherical coordinate system, the propagating direction relative to the coordinate system is constantly varying, even though the neutron does not physically change its direction. This angular redistribution [8,9] makes it difficult to handle the angular derivative term appearing in these coordinates. To overcome this phenomenon in spherical symmetric systems two different approaches are suggested. The first one is the conventional artifice of Carlson and Lathrop [8], followed by Lewis and Miller [9], and Tsai et al. [2] using the DOM, and Kim et al. [7] using the modified DOM, where a recursive relation for the coefficients $\alpha^{m\pm1/2}$ is modeled by examining the divergenceless flow conditions. Another procedure that approximates angular redistribution is a FLT-DOM by Sghaier et al. [4] and Trabelsi et al. [5], where angular streaming derivative term is derived from a series expansion of the radiative intensity on the basis of Legendre polynomials. Recently, Aouled-Dlala et al. [6] suggested a new finite Chebyshev transform (FCT) to improve the performance of the DOM when solving coupled conduction and radiation problems in a spherical or a cylindrical media.

In this work a particular implementation of the spherically symmetric FVM is introduced that applies to the problems of radiative heat transfer between two concentric spherical enclosures. The medium may be absorbing, emitting, and isotropically scattering. The gray gas assumption is implicitly used throughout the present article. The contributions of this work include (1) a new discretization scheme for spherically symmetric problems in the context of the FVM; (2) a mapping that simplifies the solution of spherically symmetric radiative heat transfer problems, thereby, spatial one-dimensional and angular one-dimensional dependence is transformed into spatial two-dimensional problems, and hence angular redistribution term is treated without any artifice to determine the coefficients; (3) a demonstration of performance of the present method. In the following, mathematical formulations and corresponding discretization equations for RTE are derived by considering the mapping procedure that describes the characteristics of the intensity in spherically symmetric coordinates by using the FVM. The present approach is then validated by comparing the present results with those of previous works.

2. Mathematical formulation

2.1. Radiative transfer equation

The geometry and coordinates for two concentric spheres are illustrated in Fig. 1, where subscripts 1 and 2 refer to each wall boundary at $r = R_1$ and $r = R_2$, respectively. $\chi = \cos^{-1}\mu$ is the angular polar angle measured from outward direction of r, ranging from 0 to π. For a radiatively active medium in a spherically symmetric enclosure as shown in Fig. 1, the r-directional radiative heat flux is defined as

$$q_r^R = \int_{\Omega=4\pi} I(\vec{r},\vec{s})(\vec{s}\cdot\vec{e}_r)\mathrm{d}\Omega \tag{1}$$

where $I(\vec{r},\vec{s})$ is the radiative intensity at position $\vec{r}$ in the direction $\vec{s}$. $\vec{e}_r$ is the base vector in the radial direction, and Ω is the solid angle. To obtain the radiative heat flux for a participating medium in a spherically symmetric coordinate, the radiative intensity at any position $\vec{r}$ along a path $\vec{s}$ through an absorbing, emitting, and isotropically scattering medium can be evaluated from the following RTE [7–9]:

$$\begin{aligned}&\frac{\mu}{r^2}\frac{\partial}{\partial r}[r^2 I(\vec{r},\vec{s})] + \frac{1}{r}\frac{\partial}{\partial \mu}[(1-\mu^2)I(\vec{r},\vec{s})]\\ &= -[\kappa_a(\vec{r}) + \sigma_s(\vec{r})]I(\vec{r},\vec{s}) + \kappa_a(\vec{r})I_b(\vec{r})\\ &\quad + \frac{\sigma_s(\vec{r})}{4\pi}\int_{\Omega'=4\pi} I(\vec{r},\vec{s}')\mathrm{d}\Omega'\end{aligned} \tag{2}$$

For a diffusely emitting and reflecting wall the above RTE is subject to the following boundary condition:

$$I_w(r_w,\vec{s}) = \varepsilon_w I_b(r_w) + \frac{1-\varepsilon_w}{\pi}\int_{\vec{n}_w\cdot\vec{s}'<0} I(r_w,\vec{s}')\mid \vec{n}_w\cdot\vec{s}'\mid \mathrm{d}\Omega' \quad \text{for} \quad \vec{n}_w\cdot\vec{s} > 0 \tag{3}$$

In Eqs. (2) and (3), subscripts w and b denote the bounded wall and black body, respectively. $\vec{n}_w$ is the unit normal vector towards medium at the spherical wall boundary, while κ_a and σ_s are the absorption and scattering coefficients of the medium, respectively.

2.2. Finite volume formulations

Spherically symmetric radiative heat transfer occurs when the intensity is independent of spatial polar angle, χ_0, and is therefore completely specified by spatial r-coordinate and angular polar angle, χ, as depicted in Fig. 1. Thereby, the intensity $I(\vec{r},\vec{s})$ is expressed as $I(r,\chi)$. The intensities denoted by I_1^1, I_2^1, I_3^1, and I_4^1 shown in Fig. 2(a) have the same radius. The spatial polar angle, χ_0, between adjacent points is $\pi/4$, where χ_0 is measured from the right horizontal line for convenience. The nodal points 1, 2, 3, and 4 are located at $\chi_0 = \pi/8$, $3\pi/8$, $5\pi/8$, and $7\pi/8$, respectively. The intensities at point 1 in Fig. 2b have the same radius, but are now all located at $\chi_0 = \pi/2$ with different angular polar angles of $\chi = \pi/8$, $3\pi/8$, $5\pi/8$, and $7\pi/8$ for intensities I_1^1, I_1^2, I_1^3, and I_1^4, respectively. Thereby it follows that I_m^1 and I_1^m have the same value of r and χ, where $m = 1$, 2, 3, and 4, therefore, $I_m^1 = I_1^m$ can be deduced. A simple mapping therefore exists between the intensities in Figs. 2a and b. Here, it is noted that the conventional DOM [2,8,9] calculates intensities I_1^m in Fig. 2b, and hence suffers

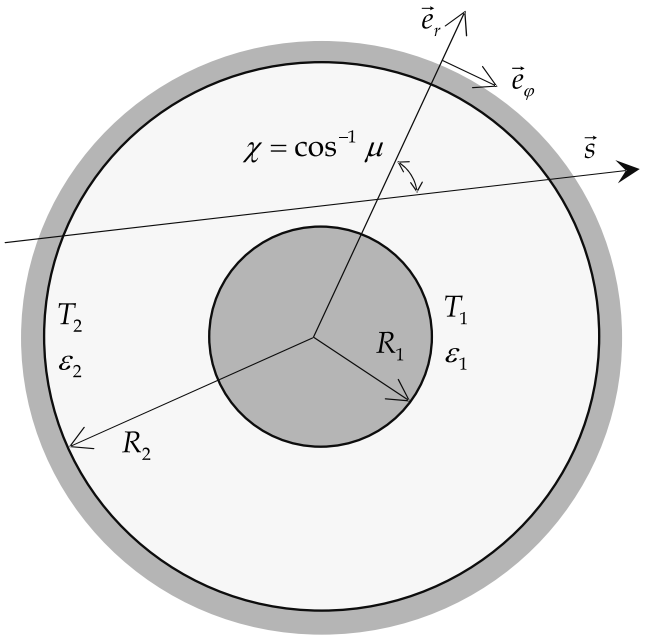

Fig. 1. Schematic of two concentric spheres and its coordinate system.

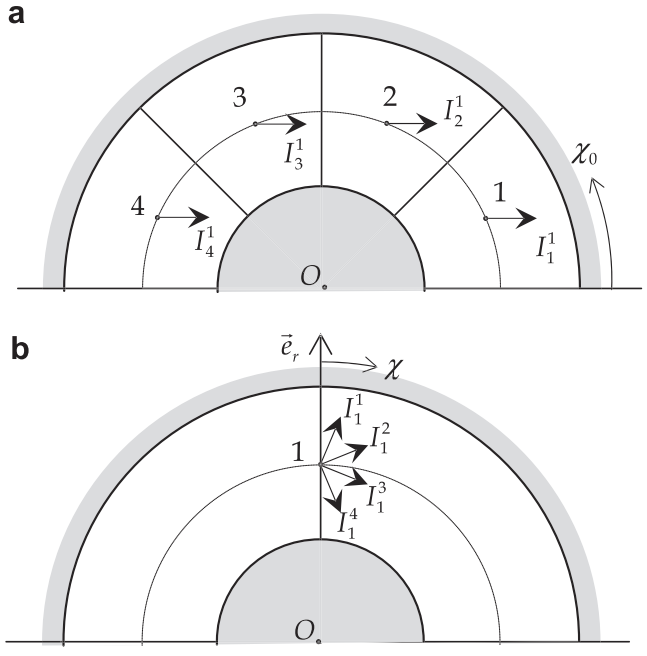

Fig. 2. Schematic of the mapping for solution of spherically symmetric radiative heat transfer between two concentric spheres. Note that I_j^k in (a) is equal to I_k^j in (b).

from a directional coupling that includes terms of angular redistribution. In this FVM, however, the intensities I_m^1 in Fig. 2a are computed, and hence, difficulties can be avoided in calculating $\alpha^{m\pm1/2}$ terms that arose from the modeling of the angular redistribution. This new treatment of angular redistribution term using spherically symmetric properties of radiative intensity can be considered as an alternative form of a novel mapping for the calculation of axisymmetric radiative heat transfer given by Chui et al. [10].

To explain the finite volume formulations in spherical enclosure, the first step is to consider the control volume adopted in this method as shown in Fig. 3, which also shows the radiative intensities at each nodal point P, E, W, N, and S with the unit normal vectors $\vec{n}_i$ at face i. The control volume represented by the nodal point P is enclosed by four control faces denoted by e, w, n, and s. This control volume shown in Fig. 3 is a ring-shaped enclosure revolving around the center point O. By using the spherical base vectors, $\vec{s} = \vec{e}_r \cos\chi + \vec{e}_\theta \sin\chi\cos\omega + \vec{e}_\varphi \sin\chi\sin\omega$, the unit normal vector at each face is expressed as $\vec{n}_i = \vec{e}_r n_{r,i} + \vec{e}_\theta n_{\theta,i} + \vec{e}_\varphi n_{\varphi,i}$, so that $\vec{n}_n = -\vec{n}_s = \vec{e}_r$ and $\vec{n}_e = -\vec{n}_w = \vec{e}_\varphi$. Fig. 4a shows the mth control angle ranging from $\chi^{m-1/2}$ to $\chi^{m+1/2}$, which is typically used in the finite volume radiation methods. The angular polar angle χ measured from the r-axis can vary from 0 to π. Here, it is noted that the angular polar angle varies as the spatial polar angle χ_0 changes, e.g., from E toward W as shown in Fig. 3, i.e. spherical base vectors for both spatial and angular coordinates, thereby, the intensities at point E and W are represented by I_E^{m-1} and I_W^{m+1}, respectively. Similarly, the intensities at face e and w are

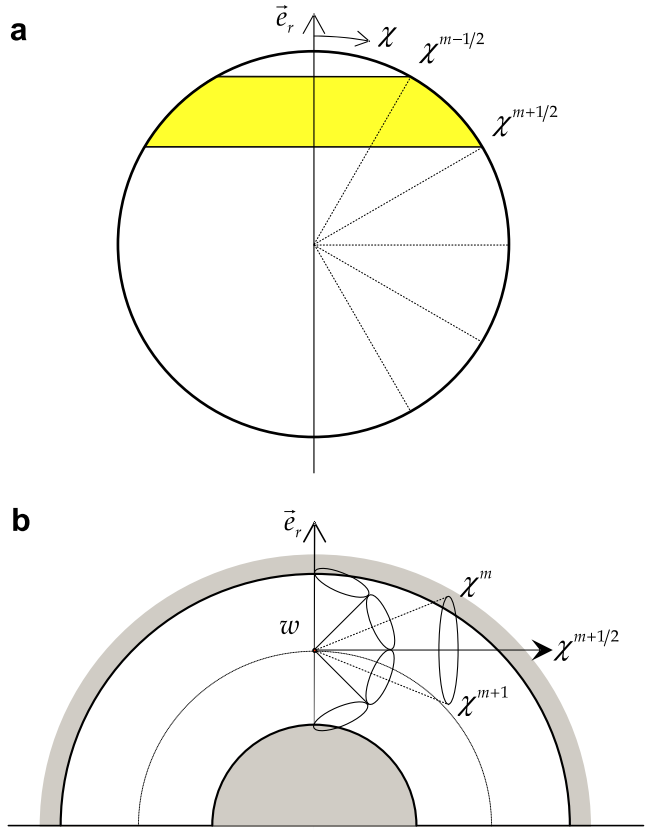

Fig. 4. Schematics of the control angle. The angular polar angle χ is measured from r-axis centered at O. Note that while the control angle χ^m ranges from $\chi^{m-1/2}$ and $\chi^{m+1/2}$, the range of angular edge control angle $\chi^{m+1/2}$ is between χ^m and χ^{m+1}.

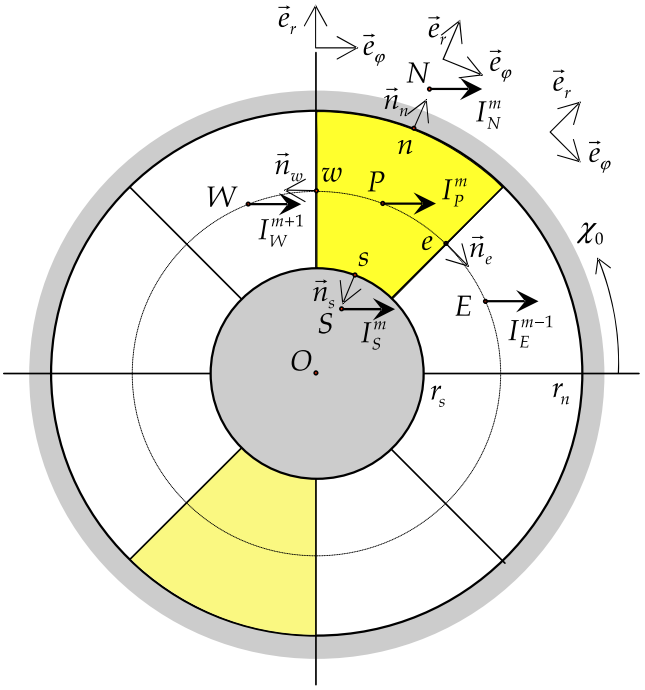

Fig. 3. Schematic of a control volume in a spherical enclosure with P located at the control volume center. The volume is a ring-shaped enclosure centered at O.

expressed by $I_e^{m-1/2}$ and $I_w^{m+1/2}$, respectively. Here, it is explained that the increment of angular polar angle is the same as that of spatial polar angle, i.e. $\Delta\chi = \Delta\chi_0$. Fig. 4b illustrates the control angle located at arbitrary point, for example, face w with total number of control angle of $N_\chi = N_{\chi_0} = 4$. The $(m+1/2)$th control angle, which is enlarged in Fig. 4b, is an edge control angle ranging from χ^m to χ^{m+1}.

Attention is now turned to the directional weights at face i through mth control angle, D_i^m, to give further explanation of the present solution method. This directional weights are defined as the inflow or outflow of radiant energy across the control volume face depending on its sign as follows:

$$D_i^m = \int_{m-1/2}^{m+1/2} (\vec{s}\cdot\vec{n}_i)\mathrm{d}\Omega = \int_{\omega=0}^{\omega=\pi}\int_{\chi^{m-1/2}}^{\chi^{m+1/2}} (\vec{s}\cdot\vec{n}_i)\sin\chi\mathrm{d}\chi\mathrm{d}\omega \tag{4}$$

where, unit direction vector, $\vec{s}$, and outward unit normal vector, $\vec{n}_i$, at face i are based on spherical coordinates explained above. Here, it is noted that the azimuthal range of control angle ω adopted is not $[0,2\pi]$ but $[0,\pi]$. The reasons are explained in detail in the following.

Based on this spatial and angular considerations, angular derivative term can be modeled by using the directional weights, which can be obtained through the integration process over a control volume ΔV and a control angle $\Delta\Omega^m$ such that:

$$\int_{\Delta\Omega}\int_{\Delta V}\frac{\partial}{\partial\mu}[(1-\mu^2)I]_{\mu=\mu^m}\mathrm{d}V\mathrm{d}\Omega \simeq \Delta A_e D_e^{m-1/2} I_e^{m-1/2} + \Delta A_w D_w^{m+1/2} I_w^{m+1/2} \tag{5a}$$

where

$$D_e^{m-1/2} = \int_{\chi^{m-1}}^{\chi^m}\sin^2\chi\mathrm{d}\chi\int_{\omega=0}^{\omega=\pi}\sin\omega\mathrm{d}\omega = (\chi^m-\chi^{m-1}) - \frac{1}{2}(\sin 2\chi^m - \sin 2\chi^{m-1}) \tag{5b}$$

$$D_w^{m+1/2} = -\int_{\chi^m}^{\chi^{m+1}}\sin^2\chi\mathrm{d}\chi\int_{\omega=0}^{\omega=\pi}\sin\omega\mathrm{d}\omega = -(\chi^{m+1}-\chi^m) + \frac{1}{2}(\sin 2\chi^{m+1} - \sin 2\chi^m) \tag{5c}$$

are the angular edge directional weights at east and west faces and $\Delta A_e = \Delta A_w = \pi(r_n^2 - r_s^2)$ is the surface area of east and west faces, respectively. It is necessary to emphasize that the angular directions $m \pm 1/2$, which appeared in Fig. 4b, are the angular edge of the control angles between $\chi^{m-1/2} < \chi^m < \chi^{m+1/2}$ and $\chi^{(m+1)-1/2} < \chi^{m+1} < \chi^{(m+1)+1/2}$, respectively. Therefore, $\Delta A_w D_w^{m+1/2} I_w^{m+1/2}$ and $\Delta A_e D_e^{m-1/2} I_e^{m-1/2}$ represent the inflow and outflow of the radiant energy through these control faces since $D_w^{m+1/2} < 0$ and $D_e^{m-1/2} > 0$ is always satisfied regardless of the spatial χ_0 location. Fig. 5 illustrates the angular edge directional weights, $D_w^{m+1/2}$ and $D_e^{m-1/2}$, with $D_n^m = -D_s^m = D_r^m$ for the case of $N_\chi = N_{\chi_0} = 4$. Here, it can be found that $D_e^{m-1/2} = -D_w^{(m-1)+1/2}$ from the geometrical point of view as shown in Fig. 5. Also, it is noted that $D_e^{1-1/2} = D_w^{N_\chi+1/2} = 0$ is always satisfied because the angular polar angle $\chi^{1-1/2} = 0$ and $\chi^{N_\chi+1/2} = \pi$, i.e. the ray direction $\vec{s}$ corresponding to $\chi^{1-1/2}$ and $\chi^{N_\chi+1/2}$ is perpendicular to the outward unit normal vector at the face $\vec{n}_e$ and $\vec{n}_w$,

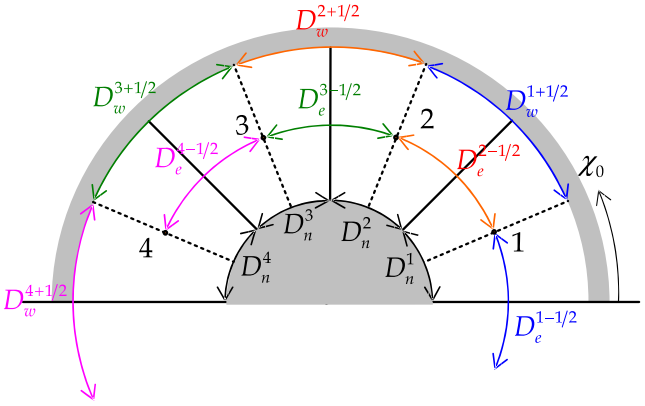

Fig. 5. Schematic representation of the directional weights for $N_{\chi_0} = N_\chi = 4$ case. Note that the directional weights, $D_n^m = -D_s^m = D_r^m$, cover n and s faces, and the angular edge directional weights, $D_e^{m-1/2}$ and $D_w^{m+1/2}$, cover e and w faces, respectively.

respectively. Thereby, $I_e^{1-1/2}$ and $I_w^{N_\chi+1/2}$ are not necessary to specify for this computation.

Now, some discussions are given below about why the integration range of azimuthal angle, ω, is chosen to be $[0,\pi]$. The first reason is to make it possible to describe the angular radiant flux through Eq. (5). If the azimuthal angle can vary from 0 to 2π, then $D_e^{m\pm1/2} = D_w^{m\pm1/2} = 0$. This means that no radiant energy is transferred across the face such as e and w in Fig. 3. The second reason is to make the radiant energy through a face totally inflow or outflow without introducing any other angular flux in the angular azimuthal direction. If the azimuthal angle varies from 0 to $\pi/2$, angular flux in azimuthal direction exists, which is not physically true in the spherically symmetric situation. The final and important reason is to avoid introducing the artifice to determine the angular coefficients, $\alpha^{m\pm1/2}$, usually adopted in the axisymmetric as well as spherically symmetric DOM. The angular directional weights, $D_e^{m-1/2}$ and $D_w^{m+1/2}$, are analogous to $\alpha^{m\pm1/2}$ in the DOM, and easily calculated from the geometric and angular grids without any assumptions usually adopted in the conventional and modified DOM.

To obtain the discretized form of the RTE, Eq. (5a) is substituted into Eq. (2), which is then integrated over a control volume, ΔV, and a control angle, $\Delta\Omega^m$, assuming that the magnitude of intensity is constant within ΔV and $\Delta\Omega^m$, but allowing its direction to vary by following the conventional practice of the FVM [10–12]. Thereby, the following equation can be obtained:

$$\sum_{i=n,s} I_i^m \Delta A_i D_i^m + [\Delta A_e D_e^{m-1/2} I_e^{m-1/2} + \Delta A_w D_w^{m+1/2} I_w^{m+1/2}] + \beta I_P^m \Delta V \Delta\Omega^m = S_P^m \Delta V \Delta\Omega^m \tag{6}$$

where $\Delta A_n = 4\pi r_n^2/N_\chi$ and $\Delta A_s = 4\pi r_s^2/N_\chi$ are the north and south surface areas, respectively. $\Delta V = 4\pi(r_n^3 - r_s^3)/3N_\chi$ is the volume of the incremental spherical shell with inner radius, r_s and outer radius, r_n, while $\Delta\Omega^m = \pi(\cos\chi^{m-1/2} - \cos\chi^{m+1/2})$ is the discrete solid angle. Note that the directional weight, D_i^m, in Eq. (4) which determines an inflow or outflow of radiant energy across the control volume face according to its sign, is evaluated as follows:

$$D_n^m = -D_s^m = D_r^m = \int_{\Omega=2\pi}(\vec{s}\cdot\vec{e}_r)d\Omega = \pi(\sin^2\chi^{m+1/2} - \sin^2\chi^{m-1/2})/2 \tag{7}$$

To relate the facial intensity, I_i^m, and the edge intensity of the angular range, $I_i^{m\pm1/2}$, to the nodal intensity, I_I^m, the following simple step scheme popularly used in the DOM and FVM is introduced to ensure positive intensity:

$$I_i^m D_i^m = I_P^m \max(D_i^m, 0) - I_I^m \max(-D_i^m, 0) \tag{8a}$$

$$I_e^{m-1/2} = I_P^m \tag{8b}$$

$$I_w^{m+1/2} = I_W^{m+1} = I_P^{m+1} \tag{8c}$$

In Eq. (8a), subscript i represents n and s, while I does the corresponding N and S. By using this scheme, Eq. (6) can be recast into the following general discretization equation:

$$a_P^m I_P^m = a_N^m I_N^m + a_S^m I_S^m + b_P^m \tag{9a}$$

where

$$a_P^m = \max(\Delta A_n D_n^m, 0) + \max(\Delta A_s D_s^m, 0) + \beta \Delta V \Delta\Omega^m + \Delta A_e D_e^{m-1/2} \tag{9b}$$

$$a_N^m = \max(-\Delta A_n D_n^m, 0) \tag{9c}$$

$$a_S^m = \max(-\Delta A_s D_s^m, 0) \tag{9d}$$

$$b_P^m = S_P^m \Delta V \Delta\Omega^m - \Delta A_w D_w^{m+1/2} I_w^{m+1/2} \tag{9e}$$

In these formulations the last terms in Eqs. (9b) and (9e) indicate the angular flux of radiant energy, which results from the modeling of angular redistribution term in Eq. (5). This completes the finite volume formulations for the calculation of radiative heat transfer in the spherically symmetric enclosure.

2.3. Supplemental equations

If there exists a nonradiative volumetric heat source, S_{nr}, in the medium, it has to be equal to the divergence of the radiative heat flux through the following radiation balance equation [13]:

$$S_{\mathrm{nr}} = \nabla \cdot q^R = \kappa_{\mathrm{a}} \left(4\pi I_{\mathrm{b}} - \int_{\Omega=4\pi} I \mathrm{d}\Omega \right) \tag{10}$$

It is noted that when the medium is in radiative equilibrium, i.e. $S_{\mathrm{nr}} = 0$, temperature distribution of the medium can be obtained directly from $4\pi I_{\mathrm{b}} = \int_{\Omega=4\pi} I \mathrm{d}\Omega$.

Once the intensity field is obtained, the radiative heat flux in the radial direction can be estimated by

$$q_r^R = 2 \sum_{m=1}^{N_\chi} I^m D_r^m \tag{11}$$

The boundary condition in Eq. (3) for a diffusely reflecting and emitting wall can be arranged to:

$$I_{\mathrm{w}}^m = \varepsilon_{\mathrm{w}} I_{\mathrm{b,w}} + \frac{1-\varepsilon_{\mathrm{w}}}{\pi} \sum_{m', D_{\mathrm{w}}^{m'}<0} I_{\mathrm{w}}^{m'} \mid D_{\mathrm{w}}^{m'} \mid \quad \text{for} \quad D_{\mathrm{w}}^m > 0 \tag{12a}$$

where

$$D_{\mathrm{w}}^m = \int_{\Omega=4\pi} (\vec{s} \cdot \vec{n}_{\mathrm{w}}) \mathrm{d}\Omega \tag{12b}$$

is the directional weight at wall. It becomes $-D_r^m$ and D_r^m at outer and inner spherical walls, respectively. The iterative solution is terminated when the following convergence criterion is attained:

$$\max\left(\left| I_P^m - I_P^{m,\mathrm{old}} \right| / I_P^m \right) \leqslant 10^{-6} \tag{13}$$

where $I_P^{m,\mathrm{old}}$ is the previous iteration value of I_P^m.

2.4. Solution procedure

To explain the solution procedure for spherically symmetric radiative heat transfer using the present method, it is helpful to revisit Fig. 2. As explained before, the intensities in Fig. 2a completely describe the spherically symmetric intensity field shown in Fig. 2b, and hence the system in Fig. 2a is considered in this work. Following the discretization procedure outlined earlier, an algebraic equation is written for the intensity in horizontal direction (i.e. $\chi_0 = 0$ direction) at each spatial node. Each nodal intensity is influenced by upstream nodal intensities.

For $\chi_0 > \pi/2$ (i.e. I_4^1 and I_3^1) the solution is marched from the outer spherical wall to the inner wall in Fig. 2a. The calculation starts from the N_χth control volume, i.e. the last control volume denoted by 4 in Fig. 2a. Along the left horizontal face no boundary face value for intensity is necessary since $D_w^{N_{\chi_0}+1/2} = 0$ as explained in the previous section. Strictly speaking, this face is not a control volume face, but only a symmetry face, therefore, no heat can physically transport across this surface. Next, the solution in the adjacent segment like the nodal point 3 can be obtained by sweeping from outer to inner wall. Here, the west nodal point intensity, I_4^1, is used as the west face intensity. This process is repeated for all segments in the left-side quadrant, $\pi/2 < \chi_0 < \pi$. The right-side quadrant, $0 < \chi_0 < \pi/2$, is similarly treated except the sweep is made from inner towards outer wall because the inner wall is in upstream direction. Here, it is noted that this solution process is somewhat similar to the works of Chui et al. [10], Moder et al. [11], and Kim and Baek [12] for the calculation of the axisymmetric radiative heat transfer.

2.5. Discussion of the finite volume formulations

As discussed by Moder et al. [11], the occurrence of angular redistribution term is determined by the choice of which angular coordinates are held fixed during the volume integration of streaming term, dI/ds, in the RTE. The spherical DOM [2,7–9] adopts the spherical base vectors as angular ones, thereby, angular redistribution terms will occur in their formulations. From this point of view, the current scheme for treating the angular redistribution term expressed in Eq. (5) can be seen as an alternative form of the works by Tsai et al. [2] and Kim et al. [7] in spherically symmetric enclosure. In the conventional [2] and modified DOM [7], angular derivative term is modeled following the conventional artifice [8,9], which maintains neutron conservation and permits minimal directional coupling:

$$\frac{\partial}{\partial \mu}\left[(1-\mu^2) I\right]_{\mu=\mu^m} \simeq \frac{\alpha^{m-1/2} I^{m-1/2} - \alpha^{m+1/2} I^{m+1/2}}{w^m} \simeq \frac{\alpha^{m-1/2} I^{m-1/2} - \alpha^{m+1/2} I^{m+1/2}}{\Delta\Omega^m} \tag{14}$$

where w^m and $\Delta\Omega^m$ is a discrete solid angle adopted in the conventional and modified DOM, respectively. And $\alpha^{m\pm1/2}$

are the coefficients for the angular derivative term to be determined. Here, a recursive relation of the coefficients for the angular derivative term, $\alpha^{m\pm1/2}$, can be determined by examining the divergenceless flow condition of Carlson and Lathrop [8] and Lewis and Miller [9] as follows:

$$\alpha^{m+1/2} - \alpha^{m-1/2} = 2\mu^m w^m = 2D_r^m \tag{15}$$

with assuming $\alpha^{1/2} = 0$ as a starting point. Then, this expression provides a recursive relation for determining the constants, $\alpha^{m\pm1/2}$. Note that, since the directional weights are analogous to the multiplication of direction cosine by quadrature weight in the conventional DOM, Eq. (5) corresponds to another form of the recursive relation [2,7–9]. In the current procedure, however, the procedure for determining the coefficients, $\alpha^{m\pm1/2}$ is not required from angular and geometric considerations as discussed earlier.

The similar solution procedure in axisymmetric radiation is found in Chui et al. [10], Moder et al. [11], and Kim and Baek [12]. In their methods, the dependence of axisymmetric intensity on two-spatial and two-angular independent variables is transformed to a dependency on three-spatial and one-angular variables by using the Cartesian base vectors for both spatial and angular treatments. Thereby, the occurrence of angular redistribution terms can be avoided. These axisymmetric solution procedures, however, cannot be applied to spherically symmetric cases because of the geometric concerns. In this work, however, the spherical spatial and angular base vectors are used, which is applicable to spherically symmetric cases.

3. Results and discussion

The solution procedures presented above are applied to pure radiative problems in two concentric spheres with various wall temperature ratio, T_2/T_1, wall emissivity, and optical thickness. For all cases presented below, equally spaced control volume of $N_r = 50$ is used. The total solid angle 2π is divided into N_χ directions with uniform $\Delta\chi$, while spatial polar angle is discretized as $N_{\chi_0} = N_\chi$ with $\Delta\chi_0 = \Delta\chi$.

To validate the present formulations for the analysis of spherically symmetric radiative heat transfer in two concentric spheres, a benchmark problem for gray absorbing, emitting, and isotropically scattering gas medium is firstly considered. Fig. 6 shows the effect of different number of angular control angle on the nondimensional radiative heat flux, $q* = q_r^R/\sigma T_1^4$, in the medium. The gray medium confined between two black concentric spheres with $R_1/R_2 = 0.5$ and $T_2/T_1 = 0.5$ is in radiative equilibrium with

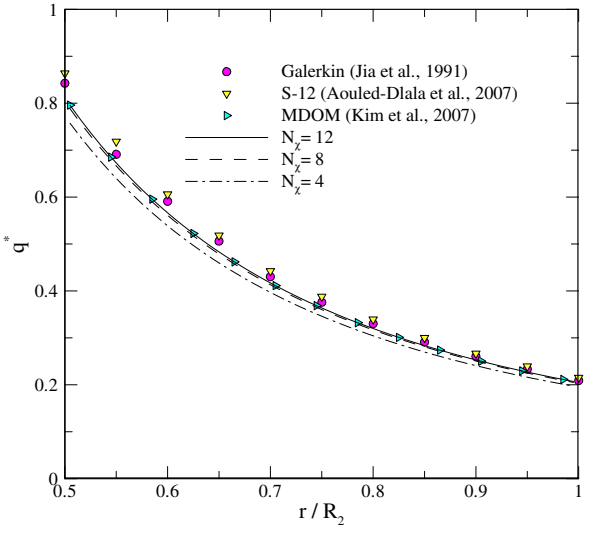

Fig. 6. The effect of angular control angle on the nondimensional radiative heat flux distribution for the case of $\varepsilon_1 = \varepsilon_2 = 1.0$, $R_1/R_2 = 0.5$, $T_2/T_1 = 0.5$, and $\tau_2 = 1.0$ with $N_r = 50$.

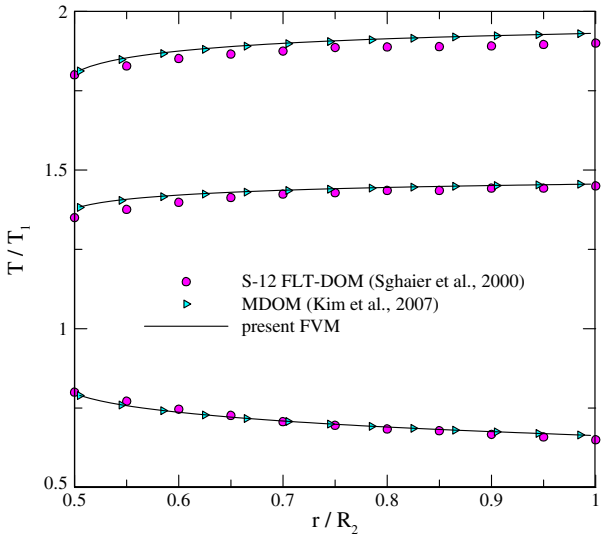

Fig. 7. The effect of temperature ratio between outer and inner spheres on the nondimensional temperature distribution for the case of $\varepsilon_1 = \varepsilon_2 = 0.5$, $R_1/R_2 = 0.5$, and $\tau_2 = 1.0$ with $N_r = 50$ and $N_{\chi_0} = N_\chi = 12$.

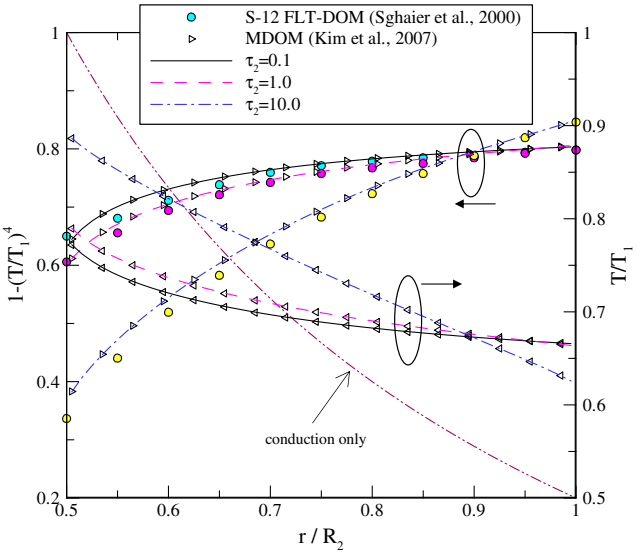

Fig. 8. The effect of optical thickness on the nondimensional temperature distribution for the case of $\varepsilon_1 = \varepsilon_2 = 0.5$, $T_2/T_1 = 0.5$, and $R_1/R_2 = 0.5$ with $N_r = 50$ and $N_{\chi_0} = N_\chi = 12$.

Table 1
Radiative heat flux for various combinations of the boundary wall temperature ratio T_2/T_1 and emissivities ε_1 and ε_2 with $R_1/R_2 = 0.5$, $\tau_2 = 1.0$, $N_r = 50$, and $N_\chi = 12$

$\frac{T_2}{T_1}$	ε_1	ε_2	$(r/R_2)^2(q_r^R/\sigma T_1^4)$				
			Galerkin ([3])	S12-DOM ([4])	S12 FLT-DOM ([4])	MDOM ($N_\chi = 12$) ([7])	Present FVM ($N_\chi = 12$)
2	1	1	−3.36557	−2.95330	−3.47938	−3.33344	−3.33625
		0.5	−2.74880	−2.47264	−2.81600	−2.72734	−2.72926
	0.5	1	−1.77357	−1.64680	−1.79980	−1.76474	−1.76643
		0.5	−1.58604	−1.49584	−1.61580	−1.57897	−1.58034
0.5	1	1	0.21038	0.18456	0.21733	0.20834	0.20827
		0.5	0.17183	0.15195	0.17281	0.17046	0.17038
	0.5	1	0.11087	0.10360	0.11312	0.11030	0.11027
		0.5	0.09914	0.09248	0.09977	0.09869	0.09866

$\tau_2 = \beta R_2 = 1.0$. As the number of control angle increases from $N_\chi = 4$ to 12, present solutions approach those of Jia et al. [2] by the Galerkin method and Aouled-Dlala et al. [6] by the FCT-DOM. Because further refinement of control angle does not significantly influence the results, $N_\chi = 12$ is adopted hereafter. It is noted in this radiative equilibrium case with isotropic scattering that the intensity distribution, the associated radiative heat flux, and medium temperature are independent of the scattering albedo of $\omega = \sigma_s/\beta$. Therefore, any set of κ_a and σ_s does not alter the results as long as $\tau_2 = (\kappa_a + \sigma_s)R_2 = 1.0$ is met.

In Fig. 7, the temperature distributions in the medium are compared with the predictions based on FLT-DOM by Sghaier et al. [4] for various wall temperature ratio of $T_2/T_1 = 2.0$, 1.5 and 0.5 for the case of $\varepsilon_1 = \varepsilon_2 = 0.5$, $R_1/R_2 = 0.5$, and $\tau_2 = 1.0$. Since only radiative heat transfer is involved, we can see that there exists the temperature jump at the bounded walls. It also shows that present predictions are in good agreement with those obtained by using the FLT-DOM. Fig. 8 shows the effect of optical thickness on the temperature profile, i.e. $1 - (T/T_1)^4$ and T/T_1. In this case, the conditions of $\varepsilon_1 = \varepsilon_2 = 0.5$, $R_1/R_2 = 0.5$, $T_2/T_1 = 0.5$ are used, while $\tau_2 = \beta R_2$ has three different values of 0.1, 1.0, and 10.0. When the medium is optically thin, the temperature of the medium is more uniform and the temperature jump near the wall is more pronounced through the far-reaching effect of radiative heat transfer. As the optical thickness increases to 10.0, the medium has steeper temperature gradient, which is closer to the profile of conduction only case [14] due to heat blockage effect of optically thick medium, hence, the temperature jump at the walls is reduced compared to optically thinner cases.

Table 1 summarizes the results of radiative heat flux of $(r/R_2)^2(q_r^R/\sigma T_1^4)$ for various combinations of the wall temperature ratio T_2/T_1 and boundary emissivities ε_1 and ε_2, and compares the present results with the other solutions by Galerkin method [3], S12 DOM and S12 FLT-DOM [4], and MDOM [7] for the case of $R_1/R_2 = 0.5$ and $\tau_2 = 1.0$. It can be seen that the present results are in a good agreement with other predictions. Finally, it is noted that the calculation time required for all the cases demonstrated in this article is less than 3 s on a 1.7 GHz Notebook computer.

4. Conclusions

Application of the finite volume method has been described for problems of radiative heat transfer between two concentric spheres separated by an absorbing, emitting, and isotropically scattering gray medium. A special discretization procedure is introduced to transform the dependence on spatial one-dimensional and angular one-dimensional intensity into spatial two-dimensional one. Thereby, angular redistribution term, which appears in such curvilinear orthogonal coordinate as cylindrical and spherical ones, is treated efficiently without any artifice usually introduced in the conventional discrete ordinates method. After a mathematical formulation and corresponding discretization equation for the RTE are derived, final discretization equation is introduced by using the directional weight, which is the key parameter in the FVM since it represents the inflow or outflow of radiant energy across the control volume faces depending on its sign. The present approach is then validated by comparing the present results with those of previous works. All the results presented in this work show that the present method is accurate and valuable for the analysis of spherically symmetric radiative heat transfer problems between two concentric spheres.

Acknowledgements

This work was supported by the Research Center of Industrial Technology at Chonbuk National University, Korea. Also, the authors would like to thank Dr. J. H. Cho in the Eco-Machinery Research Division at Korea Institute of Machinery and Materials for his constructive comments and kind help.

References

[1] R. Viskanta, A.L. Crosbie, Radiative transfer through a spherical shell of an absorbing–emitting gray medium, J. Quant. Spectrosc. Radiat. Transfer 7 (1967) 871–889.
[2] J.R. Tsai, M.N. Ozisik, F. Santarelli, Radiation in spherical symmetry with anisotropic scattering and variable properties, J. Quant. Spectrosc. Radiat. Transfer 42 (1989) 187–199.

[3] G. Jia, Y. Yener, J.W. Cipolla Jr., Radiation between two concentric spheres separated by a participating medium, J. Quant. Spectrosc. Radiat. Transfer 46 (1991) 11–19.
[4] T. Sghaier, M.S. Sifaoui, A. Soufiani, Study of radiation in spherical media using discrete ordinates method associated with the finite Legendre transform, J. Quant. Spectrosc. Radiat. Transfer 64 (2000) 339–351.
[5] H. Trabelsi, T. Sghaier, M.S. Sifaoui, A theoretical study of radiation between two concentric spheres using a modified discrete ordinates method associated with Legendre transform, J. Quant. Spectrosc. Radiat. Transfer 93 (2005) 415–428.
[6] N. Aouled-Dlala, T. Sghaier, E. Seddiki, Numerical solution of radiative and conductive heat transfer in concentric spherical and cylindrical media, J. Quant. Spectrosc. Radiat. Transfer 107 (2007) 443–457.
[7] M.Y. Kim, J.H. Cho, S.W. Baek, Radiative heat transfer between two concentric spheres separated by two-phase mixture of non-gray gas and particles using the modified discrete ordinates method, J. Quant. Spectrosc. Radiat. Transfer (2007), doi:10.1016/j.jqsrt.2007.11.009.
[8] B.G. Carlson, K.D. Lathrop, Transport theory – the method of discrete ordinates, in: H. Greenspan, C.N. Kelber, D. Okrent (Eds.), Computing Methods in Reactor Physics, Gorden and Breach Science Pub., New York, 1968, pp. 165–266.
[9] E.E. Lewis, W.F. Miller Jr., Computational Methods of Neutron Transport, John Wiley & Sons, New York, 1984, pp. 135–145.
[10] E.H. Chui, G.D. Raithby, P.M.J. Hughes, Prediction of radiative transfer in cylindrical enclosures with the finite volume method, J. Thermophys. Heat Transfer 6 (1992) 605–611.
[11] J.P. Moder, J.C. Chai, G. Parthasarathy, H.S. Lee, S.V. Patankar, Nonaxisymmetric radiative transfer in cylindrical enclosures, Numer. Heat Transfer, Part B 30 (1996) 437–452.
[12] M.Y. Kim, S.W. Baek, Analysis of radiative transfer in cylindrical enclosures using the finite volume method, J. Thermophys. Heat Transfer 11 (1997) 246–252.
[13] M.F. Modest, Radiative Heat Transfer, second ed., Academic Press, New York, 2003.
[14] F.P. Incropera, D.P. Dewitt, Fundamentals of Heat and Mass Transfer, fifth ed., John Wily & Sons, New York, 2002.